Empirical Relationship Between CME Parameters and Geo-effectiveness of Halo CMEs in the Rising Phase of Solar Cycle 24 (2011 – 2013)

A. Shanmugaraju[1] · **M. Syed Ibrahim**[1] · **Y.-J. Moon**[2] ·
A. Mujiber Rahman[3] · **S. Umapathy**[4]

Abstract We analyzed the physical characteristics of 40 halo coronal mass ejections (CMEs) and their geo-effective parameters observed during the period 2011 to 2013 in the rising phase of Solar Cycle 24. Out of all halo CMEs observed by SOHO/LASCO, we selected 40 halo CMEs and investigated their geomagnetic effects. In particular, we estimated the CME direction parameter (DP) from coronagraph observations, and we obtained the geomagnetic storm disturbance index (*Dst*) value corresponding to each event by following certain criteria. We studied the correlation between near-Sun parameters of CMEs such as speed and DP with *Dst*. For this new set of events in the current solar cycle, the relations are found to be consistent with those of previous studies. When the direction parameter increases, the *Dst* value also increases for symmetrical halo CME ejections. If $DP > 0.6$, these events produce high *Dst* values. In addition, the intensity of geomagnetic storm calculated using an empirical model with the near-Sun parameters is nearly equal to the observed values. More importantly, we find that the geo-effectiveness in the rising phase of Solar Cycle 24 is much weaker than that in Cycle 23.

Keywords Sun-Coronal Mass Ejections · Geomagnetic storms · Direction parameters

1. Introduction

It is now well established that coronal mass ejections (CMEs) from the Sun are major producers of geomagnetic storms. Especially front-sided halo CMEs were thought to be good potential candidates for producing strong geomagnetic storms (*e.g.*, Wang *et al.*, 2002;

✉ A. Shanmugaraju
ashanmugaraju@gmail.com

[1] Department of Physics, Arul Anandhar College, Karumathur 625514, Tamilnadu, India

[2] School of Space Research, Kyung Hee University, Yongin 446-701, Republic of Korea

[3] Department of Physics, Hajee Karutha Rowther Howdia College, Uthamapalayam 625533, Tamilnadu, India

[4] School of Physics, Madurai Kamaraj University, Madurai 625021, Tamilnadu, India

Zhang *et al.*, 2004; Zhao and Webb, 2003). But, as suggested by St. Cyr *et al.* (2000), not all front-sided CMEs are geo-effective. According to previous studies (Cane and Richardson, 2003; Wang *et al.*, 2002; Moon *et al.*, 2005; Gopalswamy, 2007), only about 0.5 % of all halo CMEs are geo-effective, the others are not. In addition, most of the geo-effective halo CMEs originate near the central meridian of the Sun when the locations of their associated flares are used. Mujiber Rahman, Manoharan, and Umapathy (2010) analyzed the geo-effectiveness of 91 disk-centered ($\pm 30°$) CME events and found that only 40 % of the events produced moderate ($Dst \leq -75$ nT) to severe ($Dst \leq -200$ nT) geomagnetic storms.

Using LASCO coronagraph images of CMEs and drawing an ellipse covering the entire CME brightness, Moon *et al.* (2005) introduced a direction parameter for 38 fast CME events (with a speed $v > 1300$ km s^{-1}) during the period 1997–2002. They selected 12 events to find the relationships between *Dst* and CME parameters such as mass and column density. They also found that the relation between *Dst* and direction parameter was good.

Following this study, Kim *et al.* (2008) considered 486 front-side halo CMEs observed during 1997–2003 and found that only 115 events produced geomagnetic storms at 1 AU. The direction parameter obtained using the LASCO C3 picture is more accurate than C2, so they used LASCO C3 images to find the direction parameter. The LASCO C2 and C3 instruments are externally occulted white-light coronagraphs onboard SOHO that observe Thomson-scattered visible light through a broadband filter. Similarly, Kim *et al.* (2010) investigated the relationship between the direction parameters and geomagnetic storm disturbance index. They compared the CMEs originating from source regions with northward and southward magnetic field orientations. Kim *et al.* (2010) selected 66 halo and partial halo CMEs associated with M- and X-class flares. They developed an empirical model to predict the geomagnetic storm strength. They used various CME parameters (speed, earthward direction parameter, longitude, and magnetic field orientation) to find the storm strength (*Dst*). Song *et al.* (2006) investigated 23 northward (magnetic field orientation in the source region is toward the north) CME events and found that five events produced $Dst > -100$ nT and another event produced a super storm ($Dst > -350$ nT). For these six events, the direction parameter values were greater than 0.6 (Kim *et al.*, 2008).

Forecasting geo-effective CMEs is very important. In addition, predicting the intensity of the geomagnetic storm is important to avoid the adverse effects of storms at Earth. Hence, we have selected a set of halo CMEs observed during the rising phase of Solar Cycle 24 and analyzed their geo-effectiveness. While Kim *et al.* (2010, 2013) used partial and full-halo CMEs, we have considered only full-halo CMEs. In addition, Moon *et al.* (2005), Moon, Kim, and Cho (2009), and Kim *et al.* (2008, 2010, 2013) used data from the previous solar cycle, we considered data from the present solar cycle observed during the period 2011 to May 2013. From the present study, the usefulness of the CME direction parameter in identifying geo-effective CMEs has been confirmed using data from the current solar cycle. Recently, Wang and Colaninno (2014), Kilpua *et al.* (2014) and Gopalswamy *et al.* (2014) highlighted the difference of Solar Cycle 24 to Solar Cycle 23 in producing CMEs and their geo-effectiveness. For example, Wang and Colaninno (2014) reported that Cycle 24 is not only producing fewer CMEs than Cycle 23, but these ejections also tend to be slower and less massive than those observed one cycle earlier. Gopalswamy *et al.* (2014) studied the anomalous expansion of CMEs in Cycle 24 (during December 2008–January 2014) and compared it with that of Cycle 23. They attributed the anomalous expansion to the reduced pressure in the heliosphere by ~ 40 % due to weak solar activity. Hence, we study the difference of geo-effectiveness between Solar Cycles 23 and 24. This article is organized as follows: Section 2 describes the data selection, and in Section 3 the results are discussed. In Section 4, we summarize the main results.

2. Data Selection

A total of 140 halo CME events were observed by SOHO/LASCO during the period 2011 to 2013 in the rising phase of Solar Cycle 24, as given in the online CME catalog http://www.cdaw.gsfc.nasa.gov [NASA/Goddard Space Flight Center] (Yashiro *et al.*, 2004). There are 40, 84, and 16 halo CME events in the years 2011, 2012, and 2013, respectively. Some low-mass ejections were omitted, and 40 halo CME events were finally selected using the following procedure.

We only considered the SOHO/LASCO CMEs that were classified as halo and had a speed in the range $\sim 500 \ \mathrm{km \, s^{-1}}$ to $\sim 2600 \ \mathrm{km \, s^{-1}}$ from the SOHO/LASCO online catalog. Then, we inspected SDO/AIA and LASCO images of these events, as well as their running-difference images, to determine whether they were front-side events. The flare data associated with CMEs were obtained from the online catalog at ftp://ftp.sec.noaa.gov/ [NOAA/Space Weather Prediction Center]. Geomagnetic storm disturbance index (*Dst*) values were obtained (for all the 40 halo CME events using a time window of two to four days from CME date) from the available online catalog http://wdc.kugi.kyoto-u.ac.jp/dstdir/index.html [World Data Center for Geomagnetism, Kyoto].

Multiple CME ejections and unclear storm profile data were not considered for our study. Nearly all the selected events have a one-to-one CME–storm correspondence. For the geo-effectiveness study, we associated the 40 CME events with the *Dst* index as follows. We used a drag-based model (DBM, Vršnak *et al.*, 2013; Shanmugaraju and Vršnak, 2014) to determine the arrival time of the corresponding CMEs and approximate ICME/IP shock time. Then, we examined the ACE/*Wind* data on the OMNI website and the *Dst* profile on the Kyoto website for any ICME/IP shocks and storms that occurred at the time determined from the DBM model. Time differences such as (i) DBM arrival time and IP shock time and (ii) *Dst* start time and ICME time are shown in the plots in Figure 1. Nearly 90 % of the IP shocks/ICMEs occurred within ± 24 hours of the DBM time, as shown in Figure 1a. Figure 1b also shows that *Dst* started to rise within -10 to 5 hours of the ICME start time.

We used the start time of the storm for reference because it represents the beginning of the storm disturbance after the arrival of the ICME/shock. The starting point of negative value of a geomagnetic storm is called the *Dst* starting time. Figure 1 shows that *Dst* started before the ICME arrival for 70 % of the events. In addition, *Dst* peak values were reached before the ICME starting time for 13 events in our study. This can be attributed to the fact that before the ICME is detected, the IP shock, running ahead of the ICME, strikes first the Earth magnetosphere, leading to the storm (Zhang *et al.*, 2007; Gopalswamy, 2008; Yermolaev *et al.*, 2010; Richardson and Cane, 2011). Sometimes, preceding (multiple) ICMEs produce a continuous change in *Dst* before the arrival of the ICME analyzed.

To verify that the corresponding *Dst* peak does not correspond to a corotating interaction region/high-speed stream (CIR/HSS), we have checked the interplanetary signatures according to the descriptions given in Richardson *et al.* (2006) and Choi *et al.* (2009). We found no storm due to CIR/HSS in our sample, except event number 20 in Table 1 (Keesee *et al.*, 2014).

If there were more than one *Dst* peak in the four days after the CME, we chose the one closest (within ± 24 hours) to the arrival time given by the DBM model. There are three cases (3 and 4 August 2011, 6 September 2011) in which successive CMEs might have interacted and produced a single geomagnetic storm. There are other reported cases (events on 15 February 2011 – Temmer *et al.* (2014) and Shanmugaraju *et al.* (2014); 7 March 2012 – Xie, Gopalswamy, and St. Cyr, 2013) in which the CMEs included in our study are involved in interaction with other CMEs.

Figure 1 Histogram showing the time differences in (a) difference of interplanetary (IP) shock time and transit time calculated from the drag-based model (DBM), and in (b) *Dst* start time and ICME arrival time.
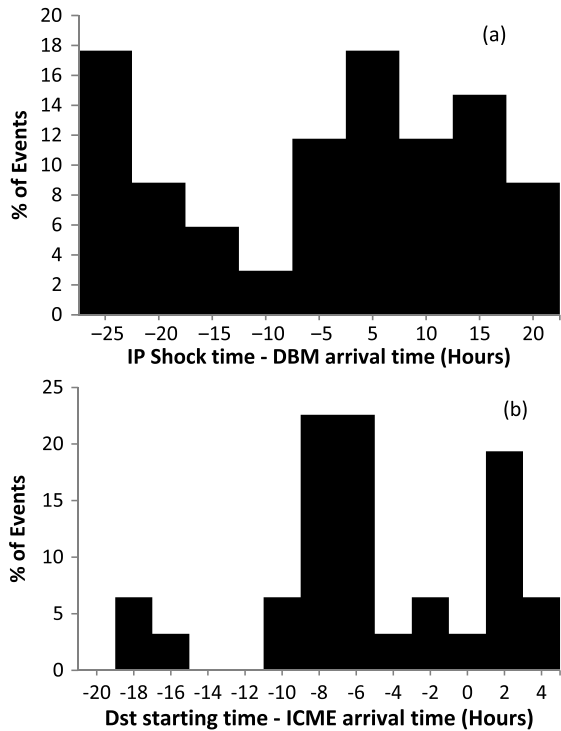
3. Results and Discussion

First, we estimated the direction parameter (DP) values of the 40 CME events. Two examples are shown in Figure 2 for the estimation of direction parameter. The direction parameter values were found using the method given by Moon *et al.* (2005): (i) we drew an ellipse around the entire CME ejection, (ii) a straight line was drawn to connect the center of the Sun and that of the ellipse, (iii) from the center of the Sun, the smaller distance to the ellipse surrounding the bright CME is '*b*' and the larger distance is '*a*'. The ratio b/a is called the direction parameter (Moon *et al.*, 2005; Moon, Kim, and Cho, 2009; Kim *et al.*, 2008).

The distribution of 40 CME events with respect to latitude and longitude of flares associated with the CMEs is shown in Figure 3. Most of the events originated from the disk center, although the distribution is broad. Of the 40 events, 23 are located between latitudes $\pm 20°$ and longitudes $\pm 30°$, and many (23/40) of the events originated on the western solar hemisphere. In this figure, a group of events in the northwestern region is marked inside an ellipse that includes nearly half of the sample. Michalek *et al.* (2006) showed that fast halo-CMEs observed up to 2002 (with true velocities higher than $\sim 1000 \ \mathrm{km \, s^{-1}}$) that originated from the western hemisphere close to the solar center caused intense geomagnetic storms. It is also known that more Earth-affecting CMEs originate in the western hemisphere (Cane and Richardson, 2003; Zhao, Feng, and Wu, 2007; Gopalswamy, 2007).

Kim *et al.* (2010) obtained the empirical relationship between the observed and calculated *Dst* for 66 full and partial halo CME events. The magnetic field orientation within a CME source region is an important factor and needs to be considered to forcast the geomagnetic storm. Assuming that the magnetic field orientation of a CME is preserved during its interplanetary transit to Earth, they found in the 66 events 42 and 24 events with a magnetic

Table 1 The details of 40 halo CME events and their geo-effectiveness. Most of them are events that originate close to the disk center. Columns 2 to 4 contain CME date, time, and speed. The associated flare location, direction parameter (b/a), geomagnetic storm values and their calculated *Dst* values are listed in last four columns, respectively.

| No.	CME			FLARE Location	GEO-EFFECTIVENESS		
	Date (dd:mm:yy)	Time	Speed (km s^{-1})		b/a	Obs. *Dst* (nT)	Cal. *Dst* (nT)
1	15.02.11	2:24	669	S20W12	0.64	−30	−47
2	02.06.11	8:12	976	S19E20	0.49	−39	−43
3	21.06.11	3:16	719	N16W08	0.63	−26	−59
4	03.08.11	14:00	610	N16W30	0.85	−107	−79
5	04.08.11	4:12	1315	N19W36	0.63	−107	−87
6	06.09.11	2:24	782	N14W07	0.36	−69	−35
7	06.09.11	23:05	575	N14W18	0.55	−69	−46
8	09.11.11	13:36	907	N24E35	0.43	−7	−50
9	13.11.11	18:36	596	N09W13	0.37	−24	−28
10	20.11.11	23:12	641	S17W42	0.31	−26	−19
11	26.11.11	7:12	933	N11W47	0.51	−44	−60
12	19.01.12	14:36	1120	N32E22	0.30	−69	−45
13	23.01.12	4:00	2175	N28W21	0.25	−73	−83
14	02.02.12	14:24	476	N08W12	0.42	−19	−28
15	29.02.12	9:12	466	N13E25	0.26	−34	−14
16	05.03.12	4:00	1531	N17E52	0.33	−74	−45
17	07.03.12	0:24	2684	N17E27	0.38	−131	−118
18	09.03.12	4:26	950	N17W03	0.77	−50	−82
19	10.03.12	18:00	1296	N17W24	0.45	−70	−67
20	26.03.12	23:12	1390	N11E01	0.47	−55	−71
21	05.04.12	21:25	828	N18E29	0.40	−31	−43
22	07.04.12	16:48	765	N14W29	0.29	−49	−20
23	12.05.12	0:00	805	N11W09	0.30	−35	−29
24	14.06.12	14:12	987	S47E06	0.81	−71	−71
25	02.07.12	8:36	1074	S18E10	0.29	−8	−30
26	11.07.12	1:25	379	S22E05	0.57	−23	−34
27	12.07.12	16:48	885	S15W01	0.92	−127	−94
28	28.07.12	21:12	420	S25E54	0.57	−27	−35
29	04.08.12	13:36	856	S19E39	0.36	−32	−41
30	13.08.12	13:25	435	N22W03	0.29	−21	−13
31	14.08.12	1:25	634	N23W08	0.33	−23	−26
32	31.08.12	20:00	1442	S19E42	0.42	−74	−72
33	28.09.12	0:12	947	N06W34	0.88	−119	−75
34	16.11.12	0:48	667	N14W29	0.35	−39	−31
35	20.11.12	12:00	619	N08E20	0.40	−38	−33
36	27.11.12	2:36	844	S12W29	0.19	−20	−14
37	05.03.13	3:48	1316	S13W48	0.54	−1	−57
38	15.03.13	7:12	1063	N11E12	0.93	−132	−104
39	11.04.13	7:24	861	N09E12	0.73	−7	−76
40	01.05.13	3:12	762	S17W36	0.27	−23	−19
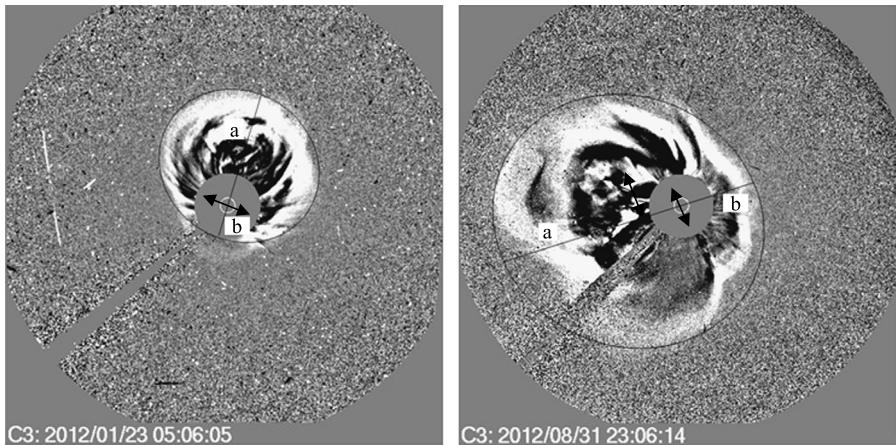
Figure 2 Halo CME events (23 January 2012 and 31 August 2012) observed by the LASCO C3 coronagraph. An ellipse is drawn to cover the entire brightness of the CME, then its symmetry axis across the center of the Sun is drawn. Along this, the longer distance from the solar center is '*a*' and smaller distance is '*b*'.

Figure 3 Plot of the location of 40 events (two events originated from the same location, N14W29). An ellipse is drawn to show a group of events in the northwestern region. It indicates that about half of the geo-effective events originated from that region.
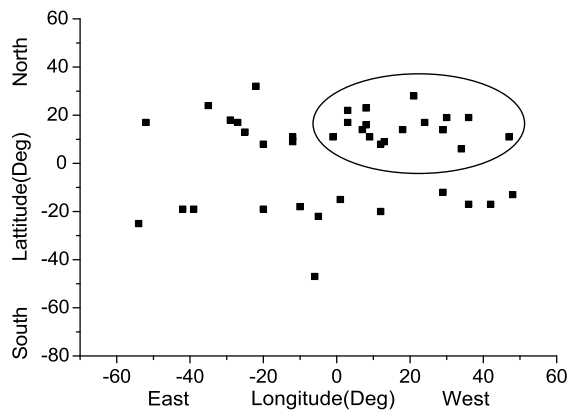
field orientation southward and northward, respectively. They deduced the empirical relationship between storm strength (*Dst*) and CME speed (*v*), direction parameter (*b/a*) and longitude (*L*) as

$$Dst = 172 - 199 \times v - 337 \times (b/a) \quad \text{[for southward events]}, \tag{1}$$

$$Dst = 47 + 53 \times L - 47 \times v - 202 \times (b/a) \quad \text{[for northward events]}, \tag{2}$$

where the CME parameters L, v, and b/a are all normalized to their maxima so that their values always lie between 0 and 1. They used these relations to forecast the storm strength and found a correlation between observed and calculated storm values for southward events of 0.66, and 0.8 for northward events. Note that Kim *et al.* (2010) found that the correlation of longitude with geo-effectiveness for southward events is negligible. Hence, they did not use parameter L in Equation (1).

To understand the relationship between CME parameters near the Sun with the geomagnetic storm strength and to use it as a forecasting tool, we correlated the CME speed and

Figure 4 Relationship between the CME plane-of-sky linear speed and the geomagnetic storm disturbance index (*Dst*).
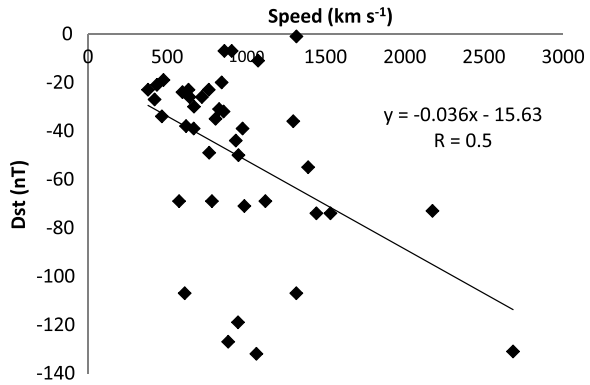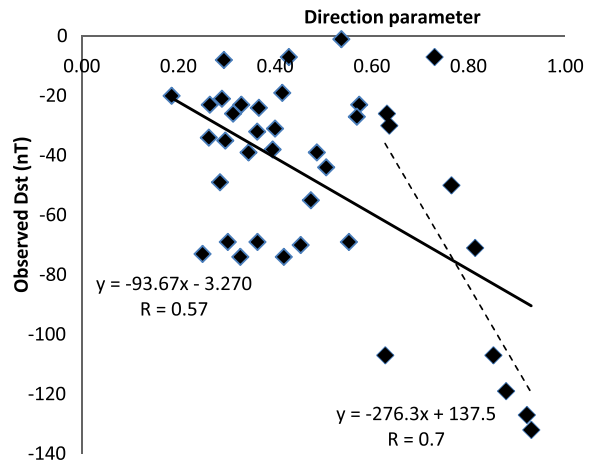

Figure 5 Relationship between observed *Dst* index and direction parameter, where the best fit for all the events is indicated as the thick line. The dashed line indicates the best fit for ten events for which *DP* > 0.6.

Dst values as shown in Figure 4. From this plot, it is clear that when the CME speed increases, the intensity of the storm disturbance increases as well. Six CME events produced a strong storm for which $Dst < -100$ nT. Srivastava and Venkatakrishnan (2004) obtained the correlation coefficient between CME speed and geomagnetic storm strength as 0.62 for the period 1996 – 2002. The correlation coefficient obtained for the present data, 0.5, is slightly lower than their value.

On the other hand, Kim *et al.* (2010) obtained the correlation between the sky plane speed and the storm disturbance value for weaker storms produced by 25 events as 0.29, significantly lower than the above correlations. From this particular analysis, we conclude that the magnitude of the storm disturbance depends only partly on the speed of the CMEs and there are some other parameters that determine the resulting *Dst* value.

The linear speed of the CMEs is not correlated with the direction parameter at all. However, the direction parameter (DP) is correlated with the storm strength. Figure 5 shows the relationship between the direction parameter and the geomagnetic storm disturbance index, and the correlation obtained is 0.57. Of the 40 events, ten events for which the direction parameter values are greater than 0.6, and the best fit for them is shown as the dashed line. For these events, the correlation is 0.7, which is slightly better than that of all 40 events (0.57). From this result, it can be understood that the geo-effectiveness of a CME also depends on the direction parameter value. Kim *et al.* (2008) showed that most of the geo-effective

events have a direction parameter value greater than 0.4. They found that when DP value increases, the *Dst* value also increases. Furthermore, Kim *et al.* (2010) investigated the relationship between storm disturbance index (*Dst*) and earthward direction parameter for 66 events whose DP value lies between 0.4 and 0.8, and they obtained a correlation coefficient of 0.6. Our result is consistent with their result: if the direction parameter value increases, the *Dst* increases as well. That is, when the direction parameter is high, the probability of the CME to have a stronger effect on the Earth's magnetosphere is higher.

We used SDO/HMI magnetograms (http://hmi.stanford.edu/data/hmiimage.html) for the CME source regions to find whether the magnetic field direction is oriented southward or northward in the CMEs. We identified the correct source active region using the flare location and found that 13 events had southward and 27 events had northward orientations. Then we used Equations (1) and (2) given by Kim *et al.* (2010) for the southward and northward events separately and calculated the storm strength (*Dst*) for the 40 events in the present study for comparison.

The data in the present work differ from their data in two ways: we used only full-halo CMEs and our study period is the rising phase of Solar Cycle 24. We developed another formula for this period. For the present data, the relation between strength of geo-effectiveness or *Dst* with CME properties (speed, direction parameter and longitude) is obtained for southward and northward events separately as

$$Dst = -84.31 \times (b/a) - 0.0276 \times V + 24.7407 \quad \text{[for southward events]}, \qquad (3)$$

$$Dst = -0.108 \times L - 100.16 \times (b/a) - 0.0417 \times V + 34.7952 \quad \text{[for northward events]}. \quad (4)$$

We obtained these relations (between the known CME parameters such as speed, direction parameter, longitude of the location, and observed *Dst*) using the multiple linear regression method of the Microsoft-excel function "Linest", which uses the least-squares method to calculate the best-fit line for a set of *y*- and *x*-values. If there are more than one independent variables, the best-fit line satisfies the equation $y = m_1 x_1 + m_2 x_2 + \cdots + b$, where *x* are the independent variables, *y* is the dependent variable, *m* are constant multipliers for each *x* range, and *b* is a constant. These empirical relations can be used to determine the unknown storm strength using the CME near-Sun parameters. When we compared the coefficients of the new equations (Equations (3) and (4)) and those of Kim's model (Equations (1) and (2)), the new coefficients were found to be different from those of Kim's equations. The deviation in the coefficients indicates that there may be a difference between the geo-effectiveness of Solar Cycle 23 and the rising phase of Solar Cycle 24. The Dst values obtained using Equations (3) and (4) are plotted against the observed *Dst* values in Figure 6a and b for southward and northward events. As seen in these plots, the correlation coefficients improved by up to ~ 0.8. Although there is a large scatter of points in the southward case, Equations (3) and (4) can be used further to compute the approximate strength of the geo-effectiveness using near-Sun parameters of CMEs. As suggested by Kim *et al.* (2010), one has to consider the real-time solar and near-Earth conditions for accurate predictions.

We also compared the *Dst* values obtained using Equations (1) and (2) with the values calculated by Equations (3) and (4) for our events here, as shown in Figure 6c and d. Although the comparison seems to be good, the magnitudes of the storm estimated using Equations (1) and (2) are much higher than those of Equations (3) and (4). This may be because the geo-effectiveness of the rising phase of Solar Cycle 24 is weaker than that of the previous solar cycle. It is similar to that of recent results. For example, Wang and Colaninno (2014) concluded that Cycle 24 not only produces fewer CMEs than Cycle 23, but that these ejections also tend to be slower and less massive than those observed one cycle earlier. Kilpua *et al.* (2014) also found that the geomagnetic activity was considerably weaker
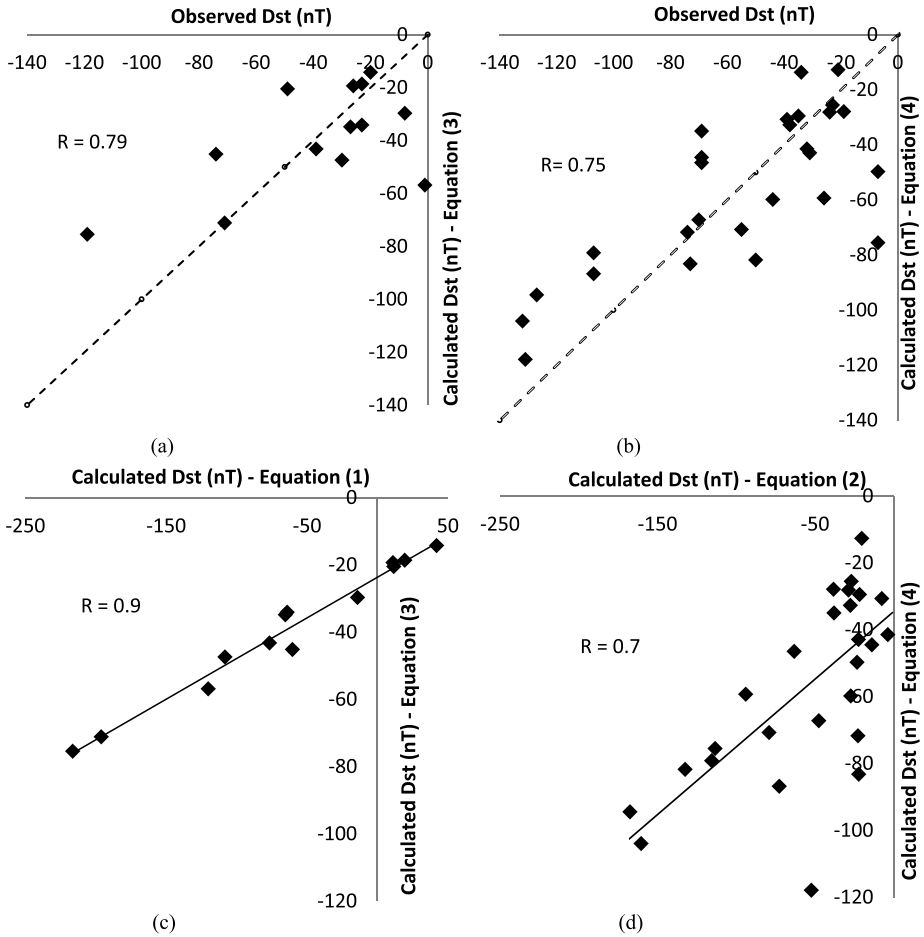
Figure 6 (a, b) Relationship between the observed and calculated *Dst* values (using Equations (3) and (4)). Dashed line denotes $y = x$. (c, d) Relationship between the calculated *Dst* values (obtained in the present study with Equations (3) and (4), and Equations (1) and (2) of Kim *et al.*, 2010). Straight line shows the best fit.

during 2006 – 2012 than during 1995 – 1999. Very recently, Gopalswamy *et al.* (2014) have observed a diminished effectiveness of CMEs in producing magnetic storms during Cycle 24 due to an anomalous CME expansion, both because the magnetic content of the CMEs is diluted and also because of the weaker ambient fields.

4. Conclusions

We selected a set of 40 CME events observed during the period 2011 – 2013 in the rising phase of Solar Cycle 24. The direction parameter and *Dst* values of all these events were obtained as described in Section 2. The relationships between the *Dst* values and other CME parameters were analyzed. The following results are obtained from our analysis:

- The relationship between the direction parameter and the *Dst* is better for Earth-directed (Sun-centered symmetric) CMEs.
- For all the 40 events, the correlation between the *Dst* values and the direction parameter is 0.6. The correlation increased up to 0.7 for events whose direction parameter was > 0.6.
- The *Dst* values and CME speed are correlated (coefficient = 0.5).
- There is no relation between the CME speed and direction parameter.
- New empirical relations were developed for southward and northward events separately to estimate the storm disturbance index (*Dst*) value using the direction parameter and speed of CMEs for the present data.
- The results were compared with the observed *Dst* index and with that given by Kim *et al.* (2010) for Solar Cycle 23. It seems that the empirical formula is strongly cycle-dependent. The geo-effectiveness in the rising phase of Solar Cycle 24 is much weaker than that in Solar Cycle 23. This difference may be caused by weaker magnetic fields in the heliosphere.
- The empirical relations obtained in our study were demonstrated as a model for predicting the intensity of the geomagnetic storm disturbance index much earlier and to forecast the geo-effectiveness in the current solar cycle.
- Nearly half of the geo-effective events are found originate from the northwestern region of the Sun.

References

Cane, H.V., Richardson, I.G.: 2003, *J. Geophys. Res.* **108**(A4), 1156. DOI.
Choi, Y., Moon, Y.-J., Choi, S., Baek, J.H., Kim, S.S., Cho, K.S., Choe, G.S.: 2009, *Solar Phys.* **254**, 311. DOI.
Gopalswamy, N.: 2007, Climate and Weather of the Sun-Earth System (CAWSES). In: Tsuda, T., Fujii, R., Shibata, K., Geller, M.A. (eds.) *Selected Papers from the 2007 Kyoto Symposium*, 77.
Gopalswamy, N.: 2008, *J. Atmos. Solar-Terr. Phys.* **70**, 2078. DOI.
Gopalswamy, N., Akiyama, S., Yashiro, S., Xie, H., Mäkelä, P., Michalek, G.: 2014, *Geophys. Res. Lett.* **41**, 2673. DOI.
Keesee, A.M., Elfritz, J.G., Fok, M.-C., McComas, D.J., Scime, E.E.: 2014, *J. Atmos. Solar-Terr. Phys.* **115**, 67. DOI.
Kilpua, E.K.J., Luhmann, J.G., Jian, L.K., Russell, C.T., Li, Y.: 2014, *J. Atmos. Solar-Terr. Phys.* **107**, 12. DOI.
Kim, R.S., Cho, K.S., Kim, K.-H., Park, Y.-D., Moon, Y.-J., Yi, Y., Lee, J., Wang, H., Song, H., Dryer, M.: 2008, *Astrophys. J.* **677**, 1378. DOI.
Kim, R.S., Cho, K.S., Moon, Y.J., Dryer, M., Lee, Y.J., Kim, K.H., Wang, H., Park, Y.-D., Kim, Y.-H.: 2010, *J. Geophys. Res.* **115**, A12108. DOI.
Kim, R.S., Gopalswamy, N., Cho, K.S., Moon, Y.J., Yashiro, S.: 2013, *Solar Phys.* **284**, 77. DOI.
Michalek, G., Gopalswamy, N., Lara, A., Yashiro, S.: 2006, *Space Weather* **4**, S10003. DOI.
Moon, Y.-J., Kim, R.-S., Cho, K.-S.: 2009, *J. Korean Astron. Soc.* **42**, 27. DOI.
Moon, Y.J., Cho, K.S., Dryer, M., Kim, Y.H., Bong, S.C., Chae, J., Park, Y.D.: 2005, *Astrophys. J.* **624**, 414. DOI.
Mujiber Rahman, A., Manoharan, P.K., Umapathy, S.: 2010, *Indian J. Radio Space Phys.* **39**, 276.
Richardson, I.G., Cane, H.V.: 2011, *Space Weather*, S07005. DOI.
Richardson, I.G., Webb, D.F., Zhang, J., Berdichevsky, D.B., Biesecker, D.A., Kasper, J.C., *et al.*: 2006, *J. Geophys. Res.* **111**, A07S09. DOI.

Shanmugaraju, A., Vršnak, B.: 2014, *Solar Phys.* **289**, 339. DOI.

Shanmugaraju, A., Prasanna Subramanian, S., Vršnak, B., Syed Ibrahim, M.: 2014, *Solar Phys.* **289**, 4621. DOI.

Song, H., Yurchyshyn, V., Yang, G., Tan, C., Chen, W., Wang, H.: 2006, *Solar Phys.* **238**, 141. DOI.

Srivastava, N., Venkatakrishnan, P.: 2004, *J. Geophys. Res.* **109**, A10103. DOI.

St. Cyr, O.C., Howard, R.A., Sheeley, N.R. Jr, Plunkett, S.P., Michels, D.J., Paswaters, S.E., Koomen, M.J., Simnett, G.M., Thompson, B.J., Gurman, J.B., Schwenn, R., Webb, D.F., Hildner, E., Lamy, P.: 2000, *J. Geophys. Res.* **105**, 18. DOI.

Temmer, M., Veronig, A.M., Peinhart, V., Vršnak, B.: 2014, *Astrophys. J.* **785**, 85. DOI.

Vršnak, B., Žic, T., Vrbanec, M., Temmer, M., Rollett, T., Möstl, C., Veronig, A., Čalogović, J., Dumbović, M., Lulić, S., Moon, Y.-J., Shanmugaraju, A.: 2013, *Solar Phys.* **285**, 295. DOI.

Wang, Y.-M., Colaninno, R.: 2014, *Astrophys. J.* **L784**, 27. DOI.

Wang, Y.M., Ye, P.Z., Wang, S., Zhau, G.P., Wang, J.: 2002, *J. Geophys. Res.* **107**(A11), 1340. DOI.

Xie, H., Gopalswamy, N., St. Cyr, O.C.: 2013, *American Astronomical Society*, SPD meeting #44, #100, 125.

Yashiro, S., Gopalswamy, N., Michalek, G., St. Cyr, O.C., Plunkett, S.P., Rich, N.B., Howard, R.A.: 2004, *J. Geophys. Res.* **109**, A07105. DOI.

Yermolaev, Yu.I., Nikolaeva, N.S., Lodkina, I.G., Yermolaev, M.Yu.: 2010, *Ann. Geophys.* **28**, 2177. DOI.

Zhang, J., Liemohn, M.W., Kozyra, J.U., Lynch, B.J., Zurbuchen, T.H.: 2004, *J. Geohys. Res.* **109**, A09101. DOI

Zhang, J., Richardson, I.G., Webb, D.F., Gopalswamy, N., Huttunen, E., Kasper, J.C., Nitta, N.V., Poomvises, W., Thompson, B.J., Wu, C.-C., Yashiro, S., Zhukov, A.N.: 2007, *J. Geophys. Res.* **112**, A10102. DOI.

Zhao, X.P., Webb, D.F.: 2003, *J. Geophys. Res.* **108**, A6. DOI.

Zhao, X., Feng, X., Wu, C.C.: 2007, *J. Geophys. Res.* **112**, 6107. DOI.